

The polarized proton source for the Harwell Proton Linear Accelerator

Autor(en): **Craddock, M.K.**

Objektyp: **Article**

Zeitschrift: **Helvetica Physica Acta**

Band (Jahr): **34 (1961)**

Heft [6]: **Supplementum 6. Proceedings of the International Symposium on polarization phenomena of nucleons**

PDF erstellt am: **21.07.2024**

Persistenter Link: <https://doi.org/10.5169/seals-513259>

Nutzungsbedingungen

Die ETH-Bibliothek ist Anbieterin der digitalisierten Zeitschriften. Sie besitzt keine Urheberrechte an den Inhalten der Zeitschriften. Die Rechte liegen in der Regel bei den Herausgebern. Die auf der Plattform e-periodica veröffentlichten Dokumente stehen für nicht-kommerzielle Zwecke in Lehre und Forschung sowie für die private Nutzung frei zur Verfügung. Einzelne Dateien oder Ausdrucke aus diesem Angebot können zusammen mit diesen Nutzungsbedingungen und den korrekten Herkunftsbezeichnungen weitergegeben werden. Das Veröffentlichen von Bildern in Print- und Online-Publikationen ist nur mit vorheriger Genehmigung der Rechteinhaber erlaubt. Die systematische Speicherung von Teilen des elektronischen Angebots auf anderen Servern bedarf ebenfalls des schriftlichen Einverständnisses der Rechteinhaber.

Haftungsausschluss

Alle Angaben erfolgen ohne Gewähr für Vollständigkeit oder Richtigkeit. Es wird keine Haftung übernommen für Schäden durch die Verwendung von Informationen aus diesem Online-Angebot oder durch das Fehlen von Informationen. Dies gilt auch für Inhalte Dritter, die über dieses Angebot zugänglich sind.

The Polarized Proton Source for the Harwell Proton Linear Accelerator

By M. K. CRADDOCK, Clarendon Laboratory, Oxford

The polarized proton source to be described has been built at Harwell for the National Institute for Research in Nuclear Science. It is to be installed on the 50 MeV proton linear accelerator at the Rutherford Laboratory there later this year.

Principle

In this source polarized protons are produced by the ionization of hydrogen atoms which have been partially polarized in passing through a strong inhomogeneous magnetic field. In a strong magnetic field, where the electron and proton spins are decoupled figure 1 shows that it is the spin state of the electron which principally determines the energies W of the hyperfine states, and their effective magnetic moments, μ_z .

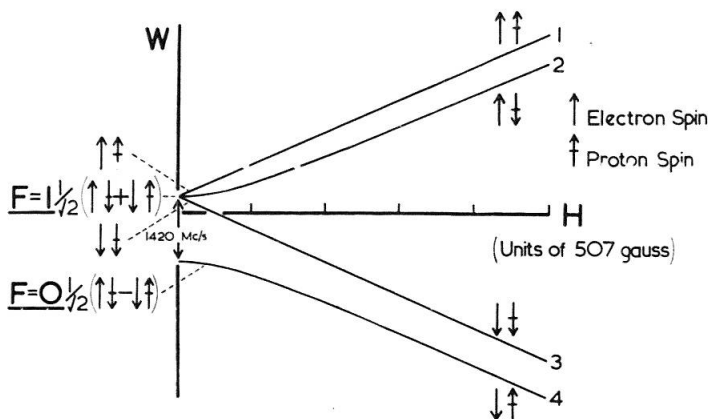


Figure 1

Energy levels of the hydrogen atom in a magnetic field

These are related by

$$W = -\boldsymbol{\mu} \cdot \mathbf{H} = -\mu_z |H|$$

and over a large range of magnetic field ($H \gg 500$ gauss)

$$\mu_z \sim \pm \mu_0$$

where μ_0 is the Bohr magneton.

Thus when the atoms are passed through a strong inhomogeneous field states 1 and 2 ($+\mu_0$) are separated from 3 and 4 ($-\mu_0$). Although the two halves of the beam are completely polarized with regard to electron spin there is as yet no proton polarization. If, however, the atoms pass into a zero field region adiabatically (i.e. without changing states) those in state 1 (1, 1) have complete, and those in state 2 (1, 0) zero proton polarization. Ionization of these atoms would thus result in a 50% polarized proton beam.

In practice ionization has to be carried out in a weak magnetic field in order to define the direction of polarization. In a field of 50 gauss the polarization is reduced to 45%.

The use of an R.F. transition at about 1500 Mc/s between states (1, 0) and (0, 0), followed by ionization in a strong field is even more promising. The transition efficiency is 75% for atoms with a Maxwellian velocity distribution and this should result in 75% proton polarization instead of 50%. Furthermore, ionization should be more efficient in a strong magnetic field.

Sextupole Magnet Principle

A sextupole magnet has been used to provide the inhomogeneous separating field. The field in an ideal sextupole, at distance r from the axis,

$$|H| = \alpha r^2$$

where α is a constant if the pole tip radius does not change.

The force acting on an atom

$$F = - \text{grad } W = \text{grad } \mu_z |H|$$

i.e. a radial force

$$F_r = \frac{\partial}{\partial r} [\mu_z |H|] = 2 \alpha \mu_z r .$$

If the field is 'strong' over most of the magnet aperture an atomic hydrogen beam will be split into two parts, one attracted to the axis, the other repelled from it, as $\mu_z = \pm \mu_0$.

If the magnet is sufficiently long the atomic beam will leave almost completely polarized in electron spin; the rejected, or 'defocused' atoms will have recombined to form molecules on the magnet surfaces, and been pumped away.

In spite of its greater complication the sextupole was preferred to a quadrupole, because of

- 1) its greater focusing power,
- 2) the simpler transition to a dipole field at the ionizer.

Both have the advantage over the dipole that they exert focusing forces on the beam of selected atoms.

Construction

The apparatus is shown diagrammatically in figure 2. Hydrogen is dissociated into atoms in a radio-frequency «ring» discharge powered by

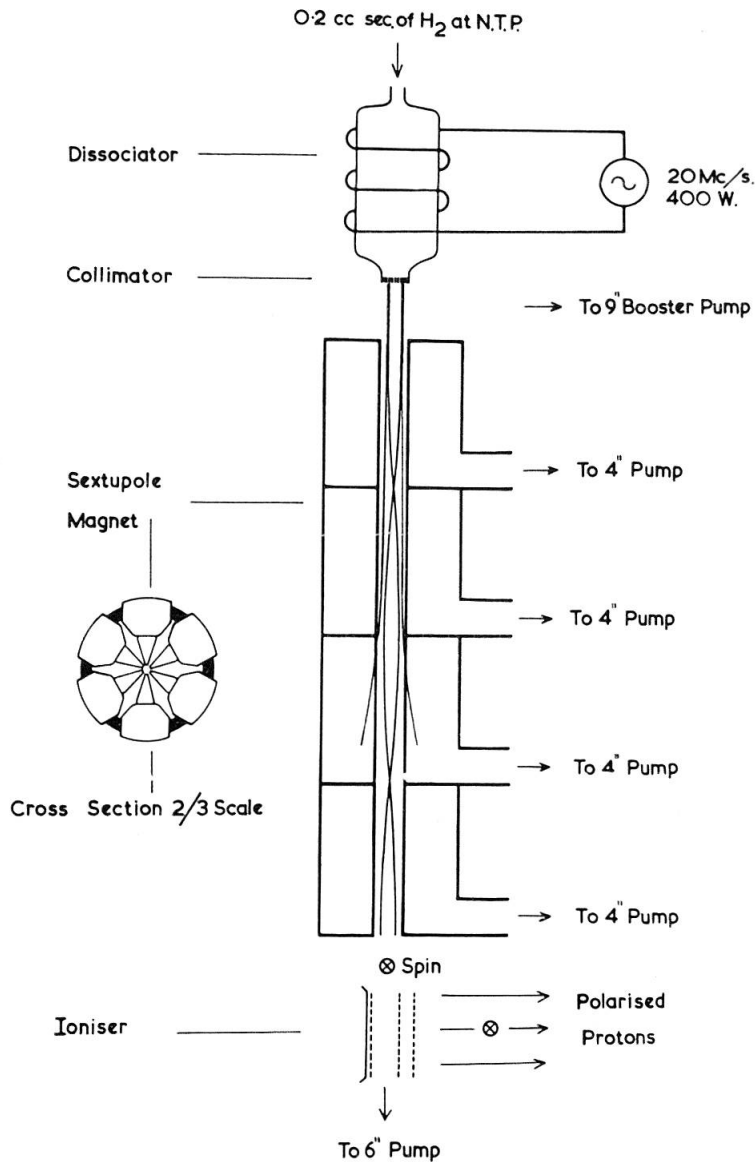


Figure 2
Schematic diagram of source

the 20 Mc/s oscillator which operates the conventional ion source. A multichannel glass 'collimator' then forms an atomic beam (90% dissociated) down the axis of the sextupole separating magnet. The polarized atoms are ionized by electron bombardment and the protons are extracted at right angles to the atomic beam and accelerated into the linac.

The resultant polarization is horizontal, but a solenoid will be used to rotate the proton spins and give vertical polarization. Then the polarization should not be affected by the beam's passage through the

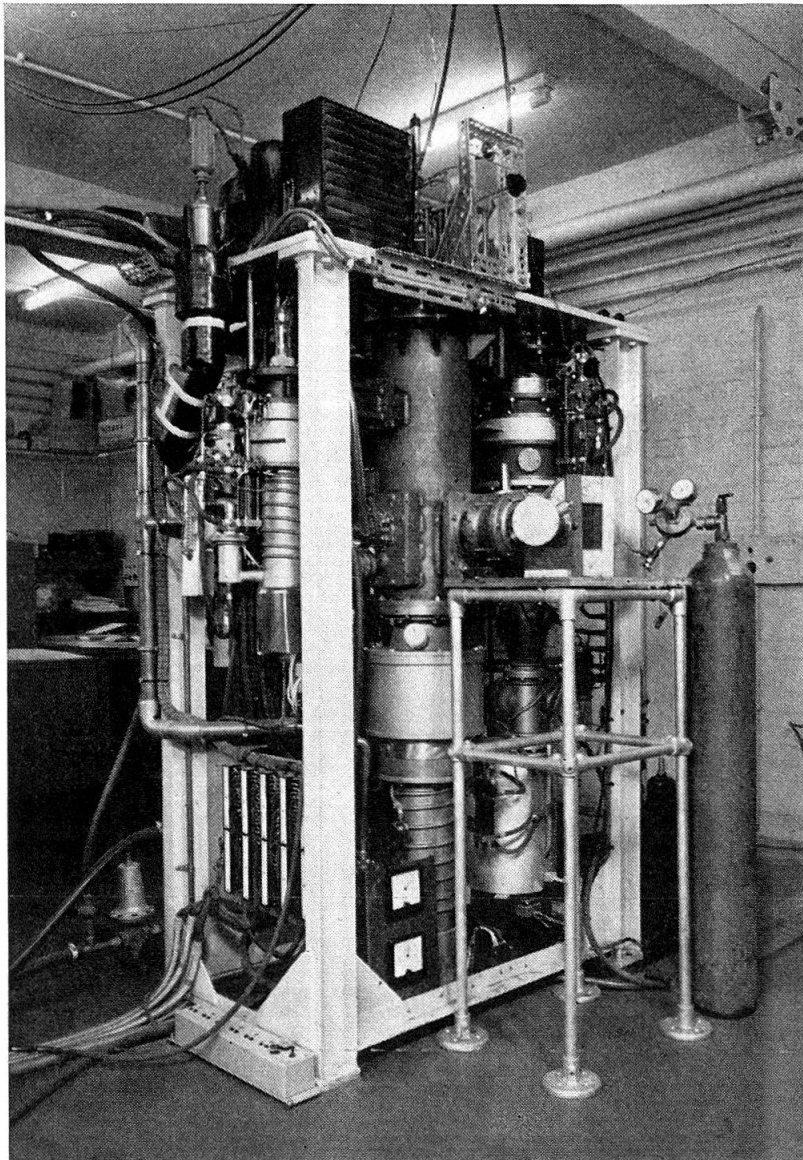


Figure 3
The polarized proton source

bending magnet, which has a vertical magnetic field and provides several radial positions for experiments on the linac. As the solenoid will be located between the ionizer and the linac injector, where the proton energy is only 1 keV, it can be short and of simple design. The combination of solenoid and bending magnet should make any direction of polarization available.

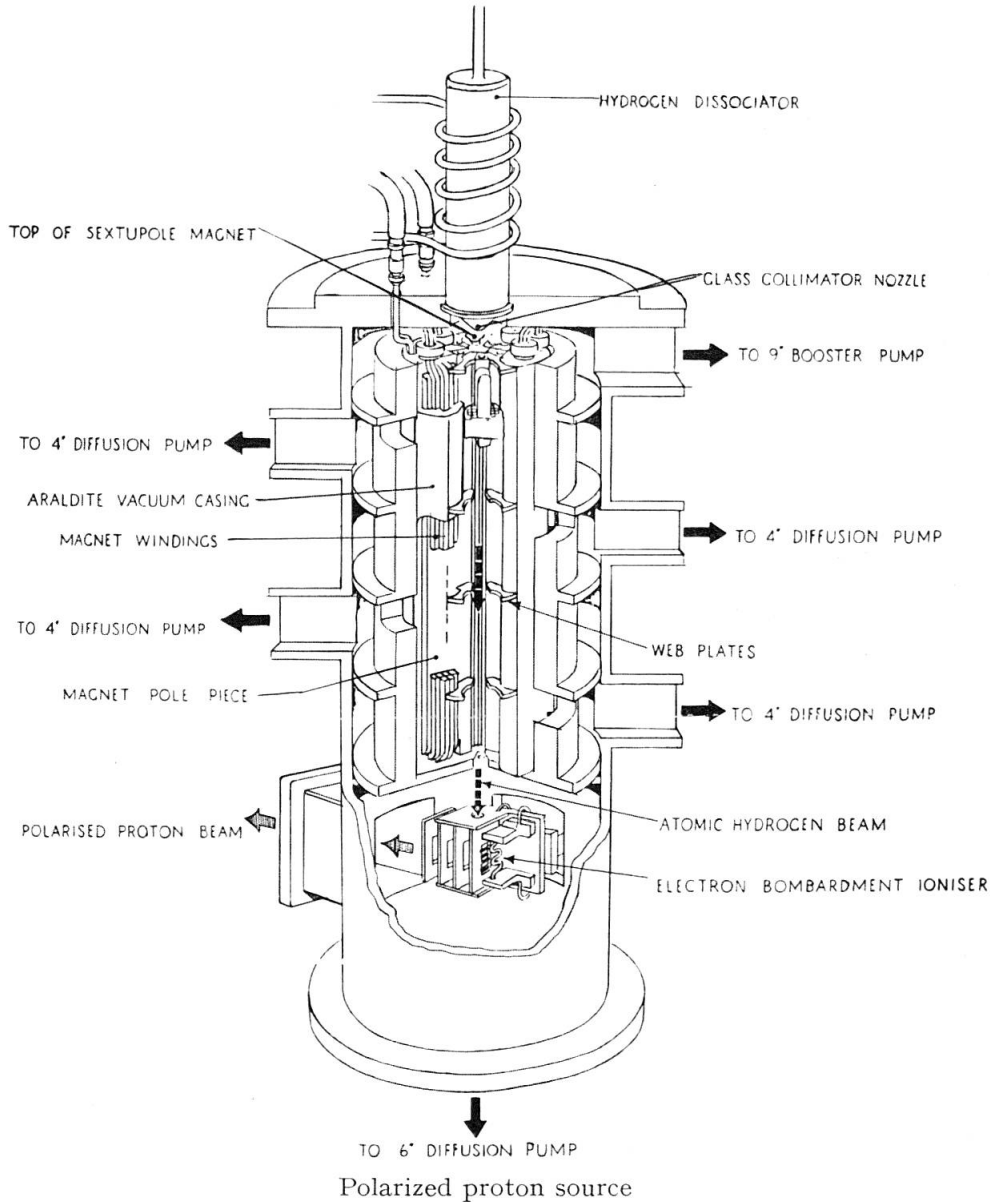


Figure 4
Cut-away diagram

Figure 3 shows the source as it appears in the laboratory. The most striking external feature is the pumping system: 6 oil diffusion pumps

and their automatic control systems and services surround the main vacuum vessel containing the magnet and ionizer.

In the laboratory experiments a simple 60° mass spectrometer has been used to distinguish the H^+ and H_2^+ components of the ion beam.

The Sextupole Magnet

Details of the magnet construction are shown in the cut-away diagram (figure 4). The poles are of mild steel, 40 cm long, and there is no shaping, the pole-tip radius being 4 mm throughout. Under running conditions the field at the pole-tips is ~ 6000 gauss, and the field gradient there 30000 gauss/cm. The exciting current of 140 A at 2 V d.c. is carried by a 1/4-inch water cooled copper tube coiled six times around each pole-piece. The windings are encased in araldite.

Proof that the separating magnet does produce polarized atoms is found in the variation of proton current from the ionizer (measured by the mass spectrometer) with sextupole field (figure 5). As the current in the magnet windings is raised to its running value of 140 A the proton current increases by a factor 4, reflecting the fourfold increase in the atomic beam under the focusing action of the sextupole.

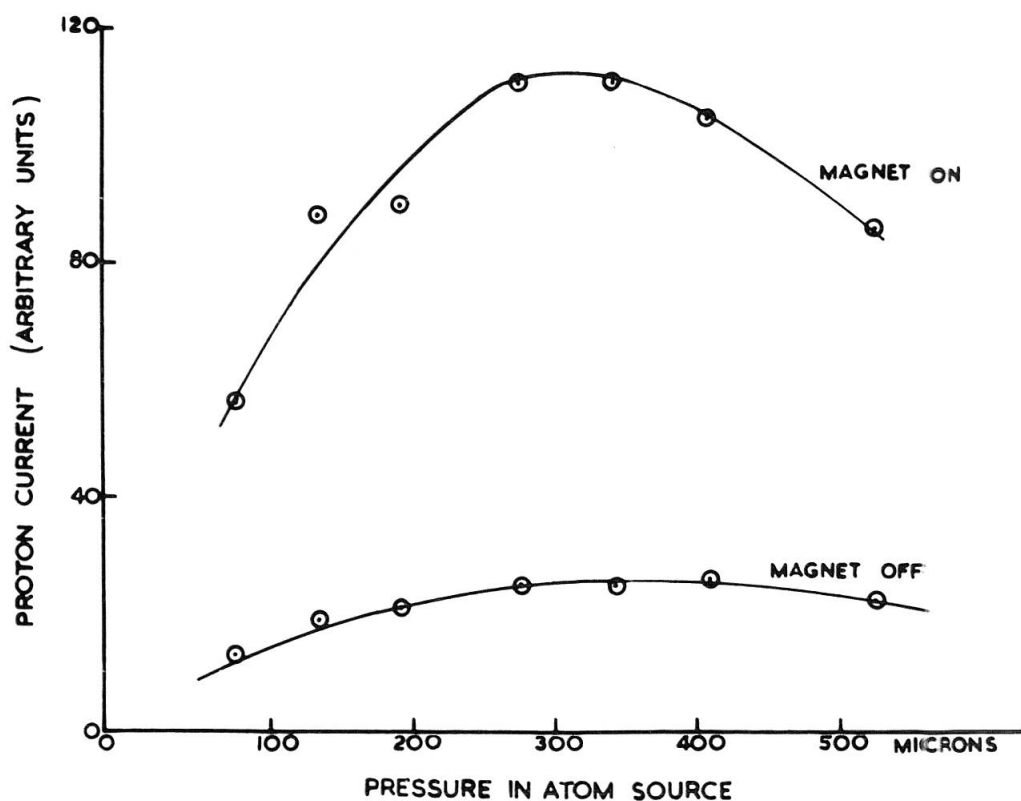


Figure 5

Proton currents - magnet on and off

Those atoms which can pass through the magnet lie within the solid angle

$$\delta\omega = \frac{2\pi\mu_0 H_m}{mv^2} \sqrt{1 - \left(\frac{r_0}{r_m}\right)^2}$$

if they enter at radius r_0 , and H_m is the field at the pole tip radius r_m . The linearity of this formula in H_m is confirmed in the linearity of the graph (figure 6). For $H_m = 6$ kg, $T = 400^\circ\text{A}$, then $\delta\omega = 2.1 \times 10^{-3}$ sterad (half-angle 1.49°), and this would suggest a focusing factor of 4.3. If the atoms leave the source at 400°A only 2% of the rejected states should be passed by the magnet and the resultant proton polarization is 48%.

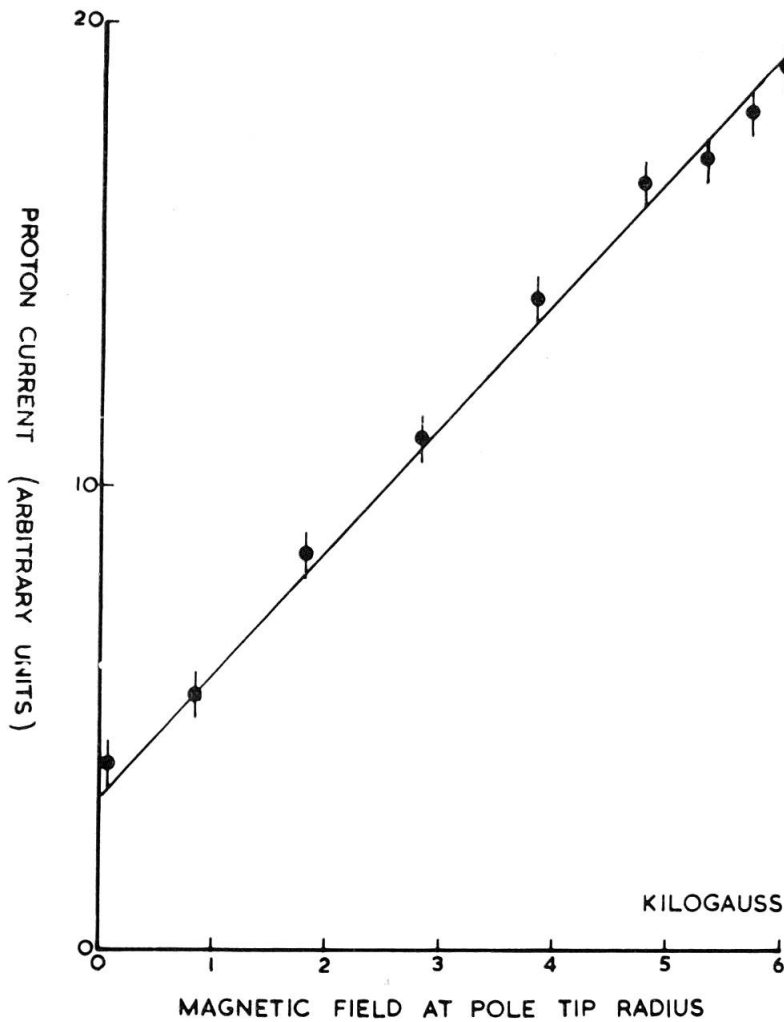


Figure 6

Focusing effect of sextupole magnet

Pumping System

The main vacuum chamber is a mild steel cylinder of 10 inches diameter. The magnet is held vertically inside this, and the space above the magnet and below the source of atoms is pumped by an Edwards 9B3 Booster pump. Most of the gas from the discharge is pumped away here and a pressure of 8×10^{-4} mm is maintained with a pressure of 340μ in the discharge. The gas flow is then $180 \text{ l}\mu/\text{s}$. Plates fitted

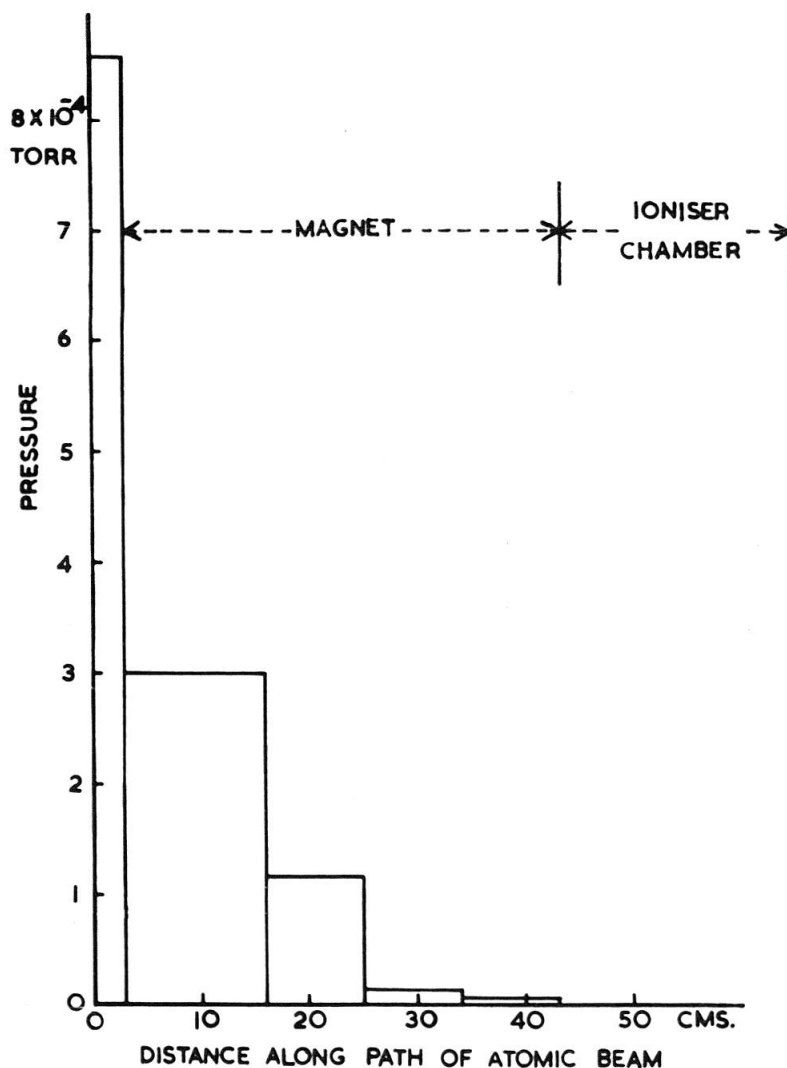


Figure 7

Residual gas pressures along the path of the atomic beam

between the pole pieces at right angles to the magnet axis divide it into four pumping sections. Each of these is pumped by an Edwards F403 oil diffusion pump. The ionization chamber, beneath the magnet, is pumped by an Edwards F603 pump. The pumping speeds of these

pumps for hydrogen are quoted by the makers as 1800, 300 and 900 l/s respectively. All these pumps are backed by a single Edwards ISC 450 rotary pump and all were originally fitted with chevron baffles refrigerated by freon at -40°C .

The residual gas pressures in the different pumping sections along the path of the beam have been estimated from the readings of ionization gauges in the pumping lines, allowing for the conductances of the pumping paths. These pressures are plotted in figure 7 for a discharge pressure of $340\ \mu$. The area under each step of the graph indicates the scattering power of each section.

By varying this 'gas thickness' it has been possible to estimate the attenuation of the beam in its passage from collimator to ionizer. Figure 8 shows a typical mass spectrometric analysis of H^+ and H_2^+ components of the ion beam, plotted against pressure in the dissociator. The beam intensity rises with dissociator pressure until the increased gas flow into the magnet chamber causes sufficient pressure rise there for the scattering to lower it again. At the optimum pressure 30% of the beam is lost by scattering.

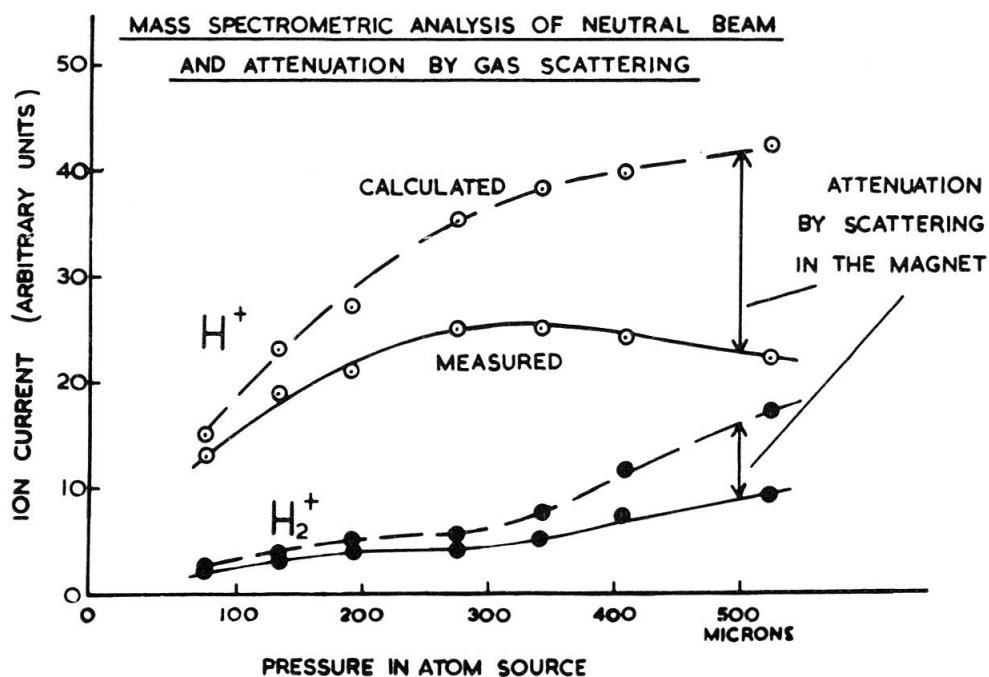


Figure 8

Mass spectrometric analysis of neutral beam and attenuation by gas scattering

The Collimator

The atomic beam is produced by a glass 'collimator' (figure 9) consisting of about 1000 capillary channels $1/8\ \text{mm} \times 2\ \text{mm}$ forming a disc

2 mm thick and of 8 mm diameter. About 35% of the disc is open to gas flow. These were made on the lines of the Born-Kessel jet used in oxygen blowpipes: the glassblower drew down capillaries, stacked them in a tube and then drew down the whole matrix to a diameter of 8 mm. This requires some practice. Collimator discs were then cut off with a diamond saw and mounted on the conical pyrex flanges (figure 10) which form the base of the discharge tube.

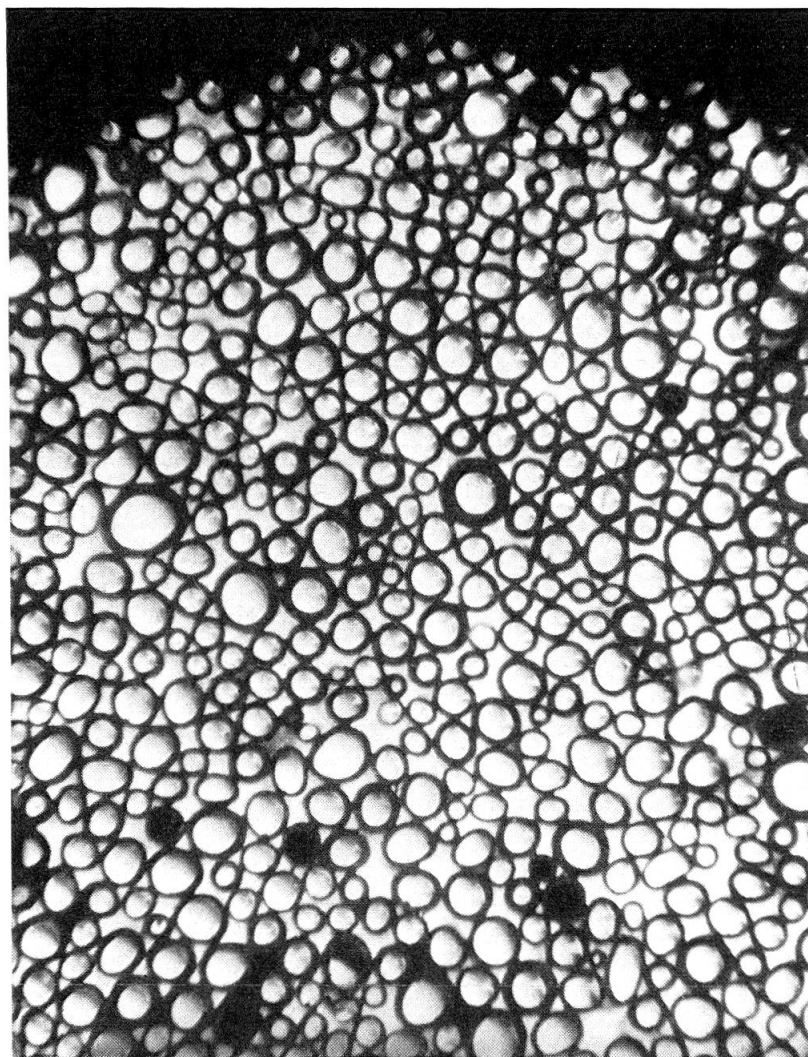


Figure 9

A section through part of the glass collimator (4 mm across)

An impression of the collimating effect of these multichannel discs is given in figure 11 where their polar diagram is compared with the cosine diagram of an infinitely thin aperture of the same area. The continuous line has been measured; the dotted part is estimated. While

the waste gas flow is reduced by a factor of more than 10 the intensity in the forward direction is not impaired. The collimator must be accurately aligned with the magnet axis.

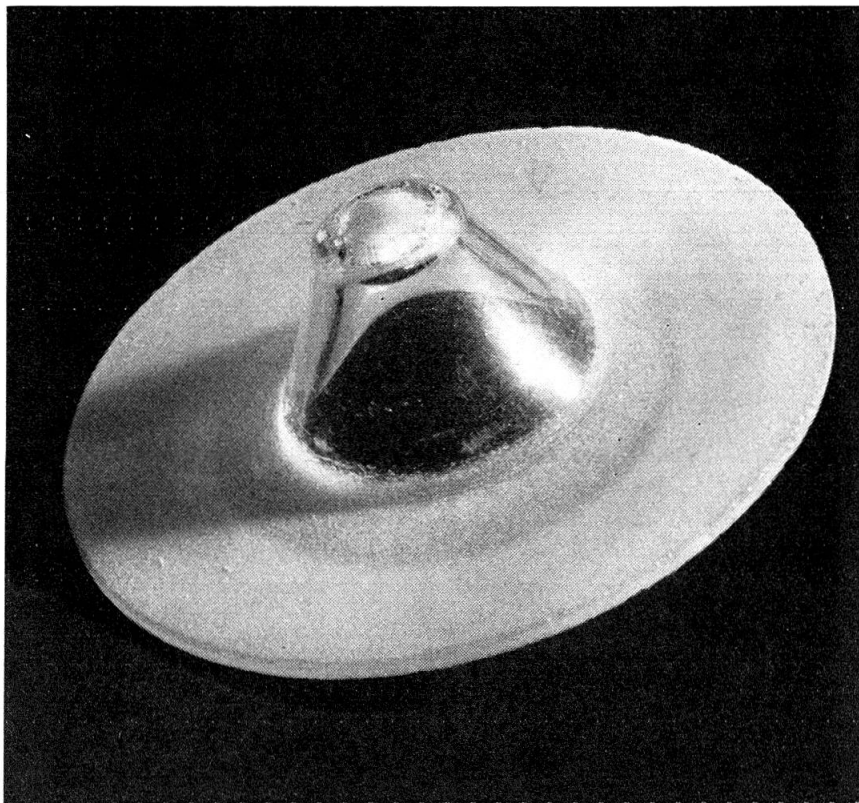


Figure 10

The collimator mounted on a 2 inch glass flange

A large single aperture of the same area could not be used in any case, for only a very low discharge pressure is allowable if molecular flow is to be maintained. The mean free path for atomic hydrogen equals the channel length, 2 mm, at a pressure of about 80μ . Contrary to expectation no decrease in beam because of cloud formation behind the collimator has been observed at this pressure; the limitation to discharge pressure, at 340μ , is attributable to attenuation of the beam by gas scattering.

The Dissociator

Pyrex glass has been used in the construction of both discharge tube and collimator; pyrex has the lowest recombination coefficient of any measured material for atomic hydrogen. Its use should result in the highest dissociation and best atomic beam for a given pressure in the dis-

charge. The tubes have furthermore been treated in various ways and the beam dissociation attainable with them is plotted against pressure in figure 12. The dissociation is calculated from the results of mass spectrometric analysis, allowing for the different ionization cross-sections of hydrogen atoms and molecules. A coating of methyl-trichlorosilane was found to be most successful, and air cooling increased the dissociation by a further 10% to over 90%.

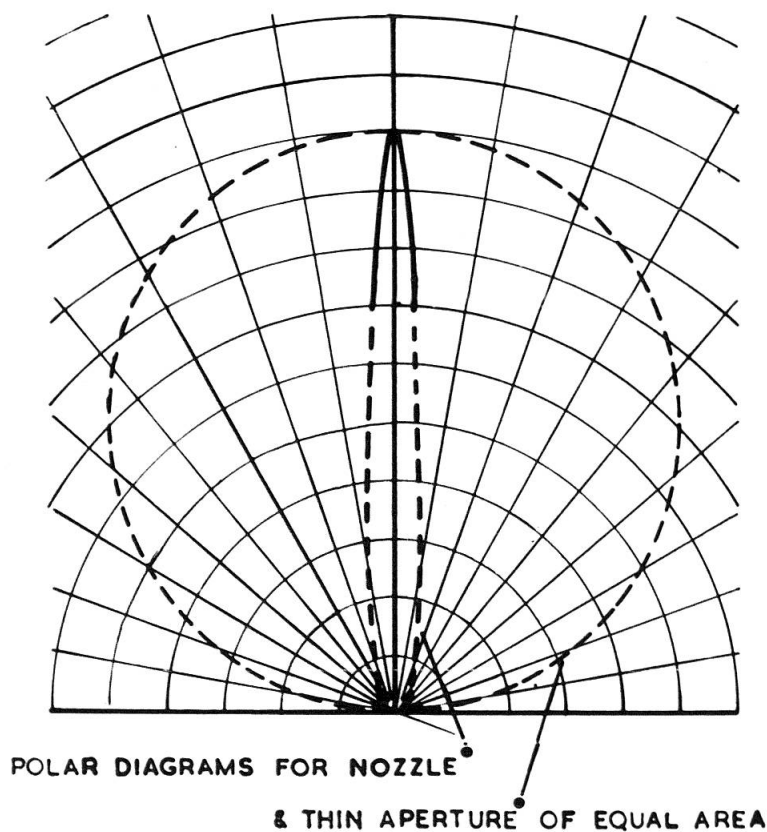


Figure 11

Collimating effect of multichannel glass nozzle

The power absorbed in the discharge has been measured roughly using a water jacket. Figure 13 shows that much more power is required at high, than at low, pressures to produce the same dissociation.

The Ionizer

This is seen in figure 14. The atomic beam, containing between 1 and 5×10^{15} atoms/s, has a 9 mm diameter and passes from left to right between the two plates nearest the camera. Electrons are drawn off the tantalum wire filament and accelerated to 250 V across a 2 mm gap

by a grid of 0.020" tantalum wires into the atomic beam. Although the nearest two plates are held at the same potential, field penetration from the further plates and the focusing effect of electron space charge cause extraction of the ion beam away from the camera. The plates are all 6×3 cm tantalum sheets with 2×1 cm holes for the beam to pass through; only the first has an actual grid of wires. Under the optimum working conditions the potentials on the filament and four plates are + 1000 V, 1250 V, 1250 V, 1200 V, 0 V respectively.

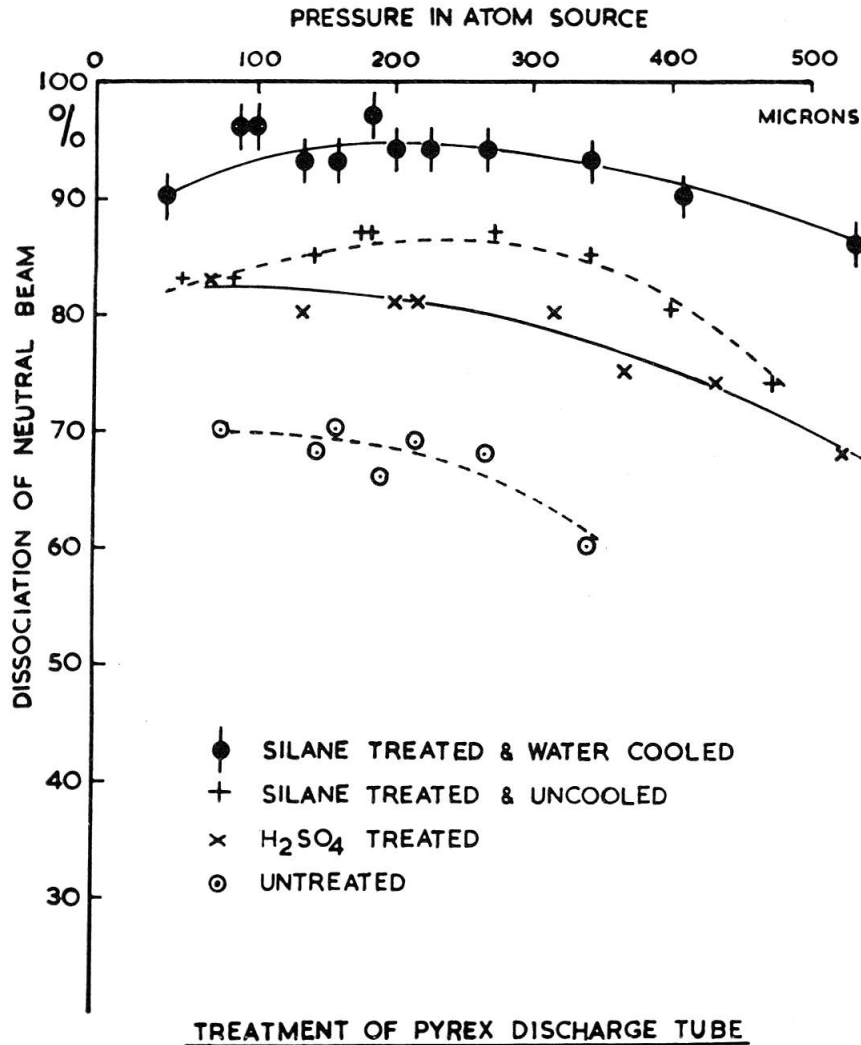


Figure 12

Dissociation of neutral beam for different treatments of discharge tube

The filament is heated to 2200° C by 36 A a.c., and about 200 mA of electrons pass through the first grid. 1 mm tantalum wire has been found to be the most reliable material; tungsten is not easily workable and oxide coated cathodes are too short-lived.

The mass analysis of the ion beam may be used to calculate the proton component of the total ion current produced by the ionizer from the neutral beam. The results of a typical measurement are given in figure 15. The best proton current there is $0.12 \mu\text{A}$ or 7×10^{11} protons/s. The efficiency of the ionizer is thus between 2 and 8×10^{-4} . The polarized proton flux available for experiments depends on how much of this can be accepted by the accelerator.

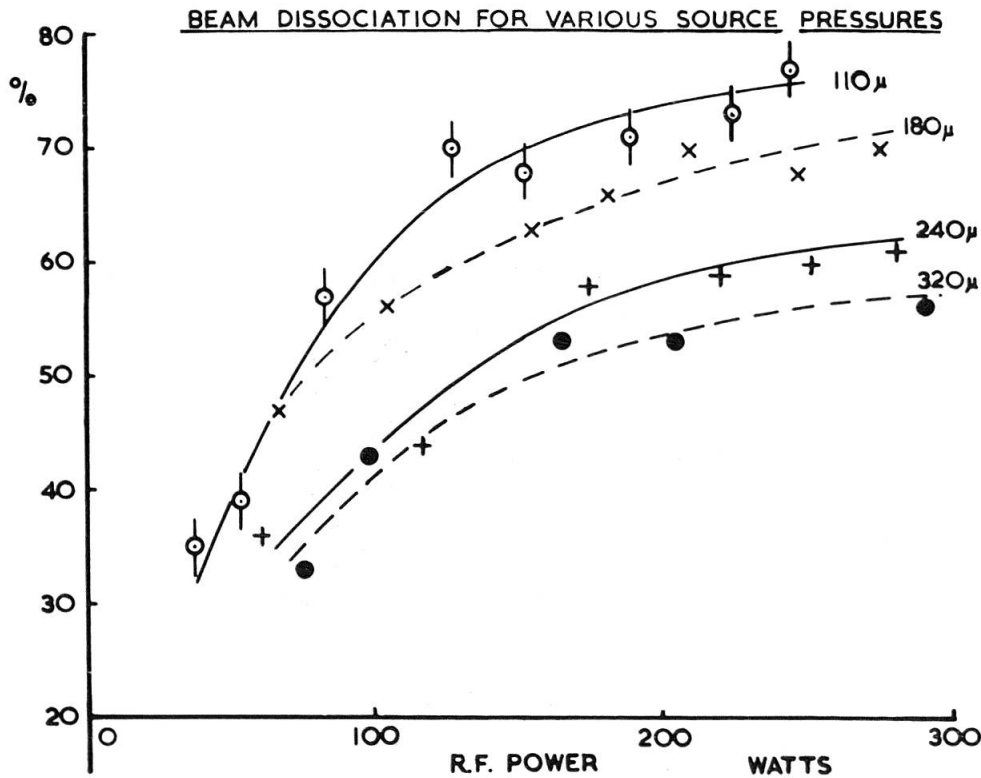


Figure 13

Dissociation of neutral beam as a function of R. F. power

Experiments on the shape of the 2×1 cm ion beam have shown that 50% of the protons travel at $< 3^\circ$ to the axis, and that it should be possible to focus 50% into the linac injector. With a transmission factor of 8×10^{-4} a mean current of 2×10^8 protons/s at 50 MeV is expected.

Background

Protons arising from the beam and from the residual gases have been distinguished using a shutter to cut off the beam. This does not alter the residual gas pressure significantly, and the difference of the two readings gives the contribution of the beam.

At first no better beam: background ratios than 1:1 could be obtained, with residual gas pressures of 2×10^{-6} mm. These protons were known not to arise from hydrogen molecules, because of the small cross-section for this process and the low population of molecules indicated by measurement of the H_2^+ current. Also, liquid-air-trapped and untrapped gauges gave quite different readings, indicating the presence of a condensible vapour. The freon baffle on the 6 inch pump was replaced by a liquid air trap, and lower pressures were obtained. No trouble has been experienced with protons from pump oil either in a test-rig or in this apparatus.

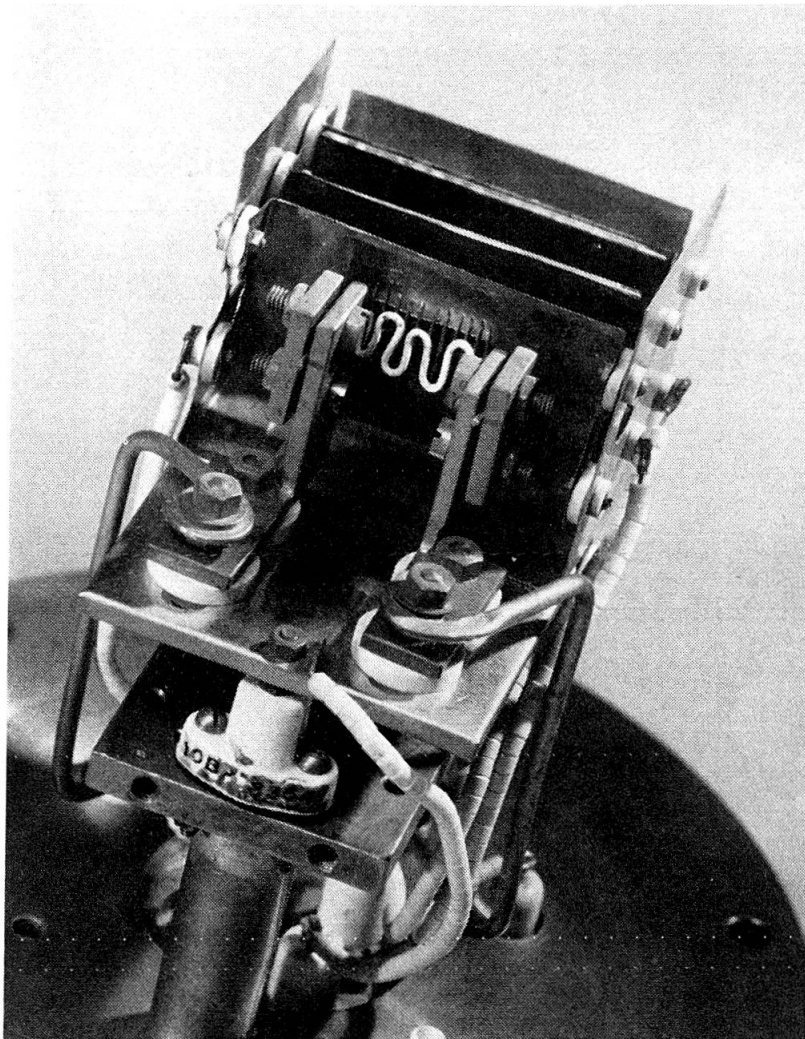


Figure 14
The ionizer

The pressure was found to rise by a factor of 3 or 4 after the ionizer had been working for a few hours. About 300 watts are dissipated by the

ionizer and the chamber walls soon reach 60°C outside. Cooling the vacuum chamber, even with an air blast was found to reduce the residual gas pressure by a factor 3. Under these conditions the pressure now rises from 2 to 8×10^{-7} mm when the ionizer is switched on and a beam: background ratio of 5:1 is obtainable (figure 16). The chamber has

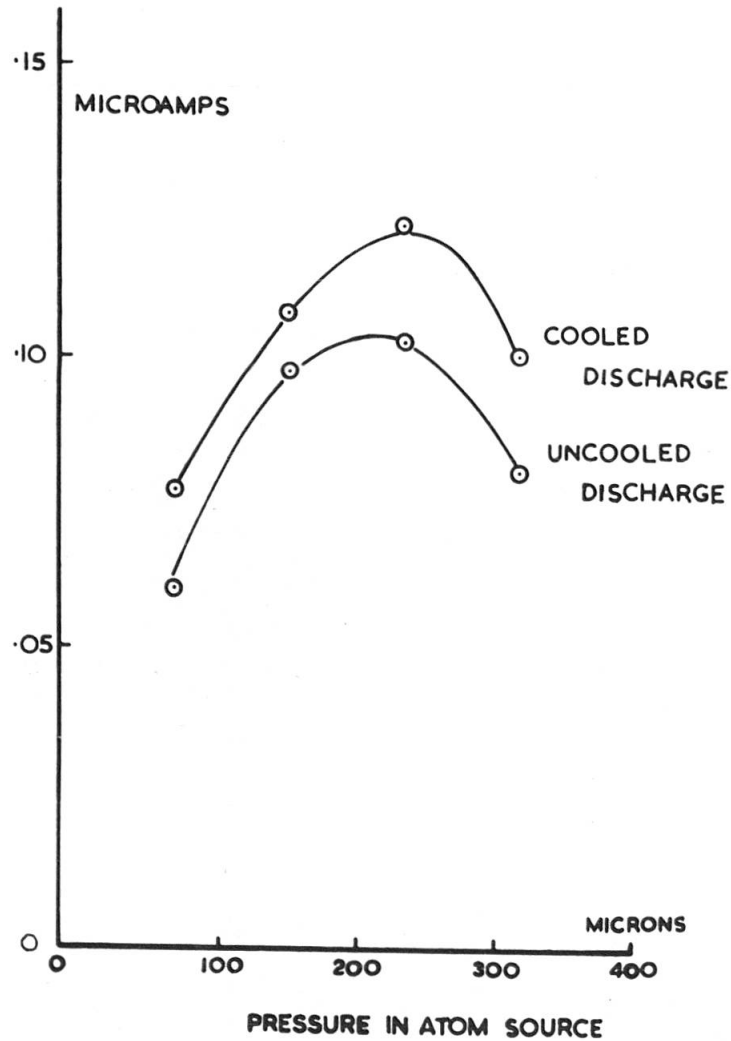


Figure 15
Total proton current

never been baked out at red heat in vacuo although it has been heated to $\sim 100^{\circ}\text{C}$ with infra red lamps, yielding considerable gas. In any future design we should use a stainless, and not mild, steel chamber. The ionizer has now been enclosed in a cooled box which will shield the chamber walls from radiation heating. It is hoped that this will improve the beam: background ratio to 10:1 but no results are yet available.

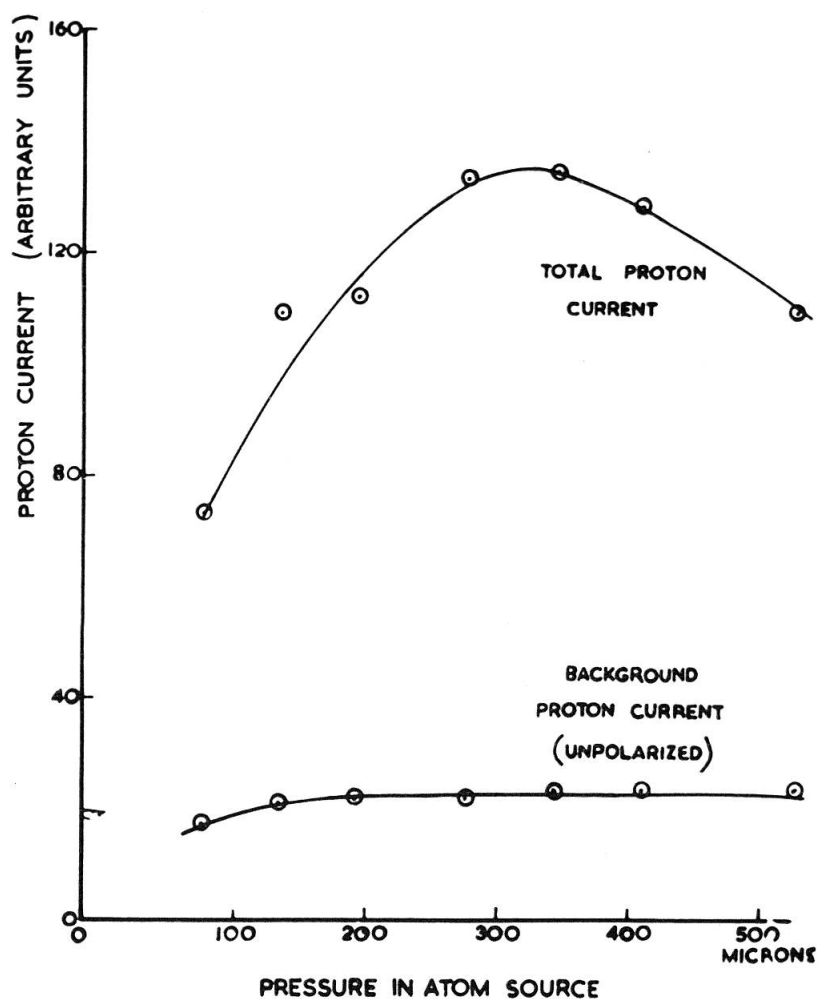


Figure 16

Proton currents from neutral beam and from background gas

Polarization

If a fraction β of the protons arise from the background the latent polarization P of the atomic beam only results in a polarization $P(1-\beta)$ of the proton beam. A 50 gauss field applied at the ionizer to swamp the stray fields of the sextupole and the filament, and define the proton spin direction, reduces the 48% polarization produced by the magnet to 43%. A background of 10% brings this down to 39%, or of 20% to 34%. It is clearly very important to keep the background and the stray fields at the ionizer as low as possible. Short of any unforeseen depolarizing action it is hoped to obtain a polarization of 40%.

Elastic scattering from He^4 at 10 MeV will be used to measure and monitor the polarization but acceleration of the beam for this purpose awaits the installation of the source on the linac.

Installation on the P.L.A.

The linac injector is supplied by a 520 kv Cockcroft-Walton H.T. generator, and the entire proton source has been designed to operate at this potential.

This has necessitated the construction of a new H.T. stand to carry the source and its associated equipment, which together weigh 2 tons. This stand will be connected to the injector by a short pipe, containing the solenoid, and which will be removable to allow conversion to a conventional ion source. This change-over should take less than 24 hours.

The services on the stand include a recirculating water chilling unit, refrigerating units for pump baffles, a traversing mechanism for beam alignment and 20 cu. ft. of electrical equipment. A 30 H.P. motor drives a 15 kW generator by belt up one of the legs of the stand; and control of the apparatus is effected by rod drive mechanisms in the legs.

Conclusion

A polarized proton source which will produce over $.1 \mu\text{A}$ of protons has been built. The polarization has not yet been measured but 40% should be attainable.

The most satisfactory points of this design seem to be

- (i) the short, strong-field magnet, which gives good intensity;
- (ii) the glass collimator which reduces the pumping requirements to a tolerable level.

The chief disadvantage is the situation of the whole source at 520 kv; however, this is outweighed by intensity considerations. The greatest opportunity for development lies with the ionizer, which has an efficiency of less than 10^{-3} .

Acknowledgements

This work has been performed with Mr. J. M. DICKSON and Mr. D. C. SALTER of the Rutherford Laboratory, and Mr. J. BOON has supervised the engineering design and construction. We are most grateful to all those in the Clarendon and Rutherford Laboratories who have contributed to the project, and to Dr. K. F. SMITH, Dr. G. H. STAFFORD and Dr. D. ROAF for many helpful discussions.